Int j simul model 23 (2024) 1, 125-136
Original scientific paper

DESIGN OF ORCHARD FERTILIZER-SOIL MIXING DEVICE BASED ON DISCRETE ELEMENT METHOD

Zhang, L. P.; Niu, X. T.; Zheng, W. Q.[#] & Cui, Z. H.
School of Mechanical Engineering, Xinjiang University, Urumchi, 830046, China
E-Mail: lyzzyjs2010@163.com ([#] Corresponding author)

Abstract
Given the uneven distribution of fertilizers of traditional orchard furrowing fertilizer spreaders, a spiral fertilizer mixing device based on furrowing fertilization was designed. The key components of the fertilizer mixing device were designed by analysing the force and movement of the particles in the proposed device. With the help of the discrete element software, an orthogonal combination test of secondary rotation was conducted for the fertilizer mixing device, with the blade angle and rotation speed of the screw auger as the test factors and Lacey index as the test index. Results shows that, when the spiral angle of the auger blade is 18° and the rotation speed of the auger is 104 r/min, the Lacey index of the fertilizer-soil mixture is 0.8 at a furrow soil thickness of 20 cm. When the soil thickness is 40 cm, the Lacey index of the fertilizer-soil mixture is 0.76, and the errors, with predicted values, of the model are 13.04 % and 9.52 %. The uniformity of the fertilizer-soil mixture of the device meets the operating requirements of furrowing fertilization and can provide a significant reference for improving the uniformity of fertilizer-soil mixtures for furrowing fertilization in orchards.
(Received in December 2023, accepted in February 2024. This paper was with the authors 2 weeks for 1 revision.)

Key Words: Fertilizer-Soil Mixing, Spiral Stirring, Lacey Index Evaluation Method, Discrete Element Method

1. INTRODUCTION

China is currently the largest fruit producer in the world, with its planting area and fruit tree output ranking first in the world. Fruit planting has become the third largest agricultural planting industry in the country, after grain and vegetable planting [1]. Orchard fertilization is an important link for promoting the growth of fruit trees. Reasonable fertilization methods play a vital role in improving the fertilizer utilization rate, fruit yield, and quality and reducing planting costs and environmental pollution [2-4]. In traditional furrowing fertilization, fertilizer-soil mixing, or full-depth mixing, is not implemented in the furrow. In addition, traditional fertilization methods do not consider the root distribution of fruit trees, which can lead to fertilizer waste and environmental pollution, to a certain extent, and trigger root burning.

Currently, scholars are focusing mainly on the design of furrowing machines with regard to orchard furrowing fertilization, in which the dominant fertilization method is trench-bottom fertilization, or whole-layer mixed fertilization, without considering fruit tree root systems. Research on fertilizer spreading discs is based mainly on field operations, which are characterized by an excessively large fertilizer spreading area and operating width. Such discs may lead to nonuniform fertilizer spreading, low fertilizer utilization rates, and failure to meet orchard fertilization quality requirements owing to their relatively poor adaptability [5, 6]. Investigations on uniform spreading in small-scale furrowing fertilization and fertilizer-soil mixing operations specific to the distribution characteristics of fruit tree root systems in the depth direction, accompanied by problems such as low fertilizer utilization rates and soil-environmental pollution, are scarce [7]. Hence, design research on fertilizer-soil mixing devices based on the distribution characteristics of fruit tree root systems may be of considerable significance to orchard furrowing fertilization.

2. STATE OF THE ART

Developed countries in Europe and the United States began studying mechanized fertilization technology at the beginning of the 20th century. In the 1970s, fertilization was basically mechanized, and the related machinery supporting the fertilization link formed in scale [8]. Fertilizer spreaders designed in developed countries feature with simple structure, wide working range, and high working efficiency. Yildirim [9] analysed the influence of the number of blades of the fertilizer spreading disc and volume flow of the fertilizer on the fertilizer spreading uniformity and provided a reference for determining the number of blades of a fertilizer spreading disc. Przywara et al. [10] analysed the effect of the fertilizer type, blade configuration of the fertilizer spreading disc, and rotation speed on the fertilizer spreading radius and uniformity. Meanwhile, the influence of the structure and working parameters of a centrifugal fertilizer spreading disc on the spatial distribution characteristics of fertilizers was clarified, and it was proven that the factors influencing the spatial distribution characteristics of fertilizers are the rotation speed of the fertilizer spreading disc, feeding position of the fertilizer, and blade angle. Villette et al. [11] analysed the influence of the fertilizer discharge rate and rotation speed of the fertilizer spreading disc on the outlet angle and radial mass distribution of fertilizer. The results showed that as the fertilizer discharge rate increases, the change trend of the outlet angle depended on the type and rotation speed of the fertilizer spreader, and the average value of the radial mass distribution decreases as the speed and flow increase.

Research on orchard fertilization machinery has a late start in China, with the relatively weak development and low mechanization level of such machinery [12, 13], which mostly adopted the operating mode of mechanical furrowing and artificial assisted fertilization. Through continuous introduction, digestion, and absorption in recent years, a relatively mature furrowing fertilization operation system was gradually established. Huang [14] developed a traction-type fertilizer mixing and backfilling device for orchard furrowing fertilization that integrated furrowing, fertilizing, fertilizer mixing and backfilling, and realized whole-layer fertilizer-soil mixing in the furrow. Sun [15] designed a suspended layered fertilizing machine for orchards that realized layered furrowing fertilization by adjusting the height of the fertilizer outlet. Zhang [16] developed a suspended fertilizing machine with precise control over fertilizer-soil mixing for fruit trees that used a soil collector to collect the soil discharged from furrowing, then mixed the fertilizer with the soil through the auger in a fertile-soil cylinder to achieve the effect of whole-layer fertilizer-soil mixing. Cai and Zhao [17] analysed the blade structure of a double-helix conical mixer and studied its influencing law on the particle mixing effect. Xiao et al. [18] designed a double-helix fertilizing machine for orchards and investigated the parameters of the spiral blades that affected the tillage resistance.

To sum up, existing research on orchard furrowing fertilization machinery focused mainly on furrowing, with furrow bottom fertilization, or whole-layer mixed fertilization, as the dominant fertilization method, and was not specific to fruit tree roots. Meanwhile, research on fertilizer spreading discs was based mainly on field operations and rarely investigated uniform fertilizer spreading in the furrowing fertilization of small areas and soil-fertilizer mixed operating devices based on the distribution characteristics of fruit tree root systems in the depth direction, accompanied by problems such as low fertilizer utilization rates and soil-environmental pollution. Therefore, in this study, a spiral soil-fertilizer mixing device is designed to solve the problem of nonuniform fertilizer spreading and nonspecificity of existing fertilizer-soil mixing devices to crop root systems and provide a reference for the study of fertilizer-soil mixing devices.

The rest of this study is organized as follows: in section 3, the key components of the fertilizer-soil mixing device are designed and modelled to complete the simulation of the fertilizer mixing process of the proposed device, and in section 4, the fertilizer-soil mixing

simulation results are analysed, and the theoretical study results are verified. In the final section, the entire study is summarized, and relevant conclusions are drawn.

3. METHODOLOGY

3.1 Structure and working principle of fertilizer-soil mixing devices

The fertilizer-soil mixing device mainly involves two processes: fertilizer discharging and fertilizer-soil mixing (Fig. 1). When the device is turned on, the furrowing device performs the furrowing operation, and the quantitative soil covering device fills the furrow with soil up to a certain depth. Meanwhile, the fertilizer is spread evenly on the surface of the covered soil in the fertilizer discharging process, then the fertilizer and soil are stirred and mixed in the fertilizer-soil mixing process. Finally, the backfilling mechanism performs the soil backfilling operation to complete the fertilizer mixing process.

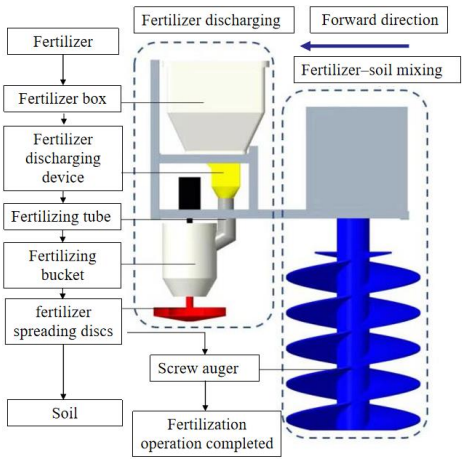

Figure 1: Fertilizer-soil mixing device.

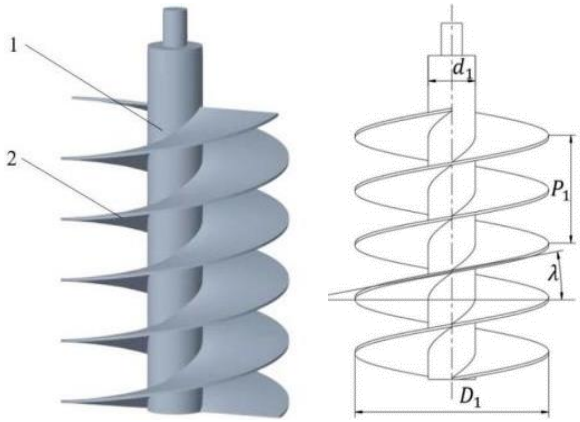

Figure 2: Structural parameters.

3.2 Parameter design of key components of fertilizer-soil mixing device

According to the agronomic requirements of orchard furrowing fertilization, the furrowing depth and width are generally required to be 0.2–0.6 m and 0.3–0.5 m, respectively, and the densest part of the crop roots should typically be within a depth range of 0.2–0.6 m. Therefore, the depth required by the fertilizer-soil mixing device is 0.2–0.6 m, that is, the fertilizer-soil mixing operation requires a minimum soil thickness of around 0.2 m and maximum soil thickness of around 0.4 m.

Structural parameter design of spiral auger: The screw auger, which is a key component of the fertilizer-soil mixing device, is composed mainly of a screw shaft and blade (Fig. 2). In the fertilizer-soil mixing operation, the screw auger rotates to realize the mixing between the soil and fertilizer particles. The particles move relatively under the action of the supporting force, friction force, gravity, and centrifugal force to realize the soil-fertilizer mixing. The blade of the spiral auger can be regarded as a helicoid consisting of numerous spiral lines. The spiral equation of the edge of the blade is:

$$\begin{cases} \mathrm{x} = c\cos\beta \\ y = c\sin\beta \\ z = \dfrac{P_1}{2\pi}\beta \\ \dfrac{d_1}{2} \le c \le \dfrac{D_1}{2} \\ 0 \le Z \le 0.5 \end{cases} \tag{1}$$

where: β is the polar angle of the spiral line, c is the maximum diameter difference of the spiral line, P_1 is the blade lead of the spiral auger, d_1 is the shaft diameter of the spiral auger, D_1 is the spiral outer diameter of the spiral auger, and λ is the blade angle of the spiral auger.

The relationship between the lead and diameter of the spiral auger can be expressed as the spiral angle, and its relationship with the lead and outer diameter of the spiral auger is as follows:

$$\lambda = \arctan\frac{P_1}{\pi D_1} \tag{2}$$

Among them, the spiral outer diameter D_1 is 0.36 m, based on the furrowing width (0.4 m) of the orchard furrowing fertilization machine. The height of the spiral agitator should be no less than 0.5 m, according to the soil-fertilizer operating requirements. The other parameters, such as the spiral shaft diameter d_1 and screw pitch P_1 are determined after the spiral auger is analysed.

Motion characteristic analysis of fertilizer particles: The movement of the particles on the blade of the screw auger is affected by not only the shear and squeeze actions of the spiral auger but also the shearing action between the particles. thus, only one particle is selected for analysis in this study. The particle is assumed to be a rigid particle, with a mass of m, and the spiral angle difference at the same radial direction of the spiral auger and interaction between the air and particles are ignored. A spatial coordinate system is established, with the intersection of the central axis of the spiral auger and bottom surface of the spiral auger as the origin and the central axis of the spiral auger as the z-axis. The particle moves along the blade, and the stress situation at a certain point is shown in Fig. 3, where n is the normal of the spiral auger blade at the particle position, t is the tangent of the spiral auger blade at the particle position, and X′ is the projection of the x-axis on the XOY plane, where the particle is located. The stress equation of the fertilizer particles is established, as follows:

$$\begin{cases} F_l = m_j^2 c \\ F_N = mg\cos\lambda \\ F_f = \mu mg\cos\lambda \\ G = mg \end{cases} \tag{3}$$

where c is the maximum diameter difference of the spiral line, λ is the blade angle of the spiral auger, ω_j is the angular velocity of the spiral auger, G is the gravity of the particle, F_l is the centrifugal force of the particle at the position, F_N is the supporting force of the particle, F_f is the friction force of the particle, and μ is the friction coefficient between the particle and spiral auger blade.

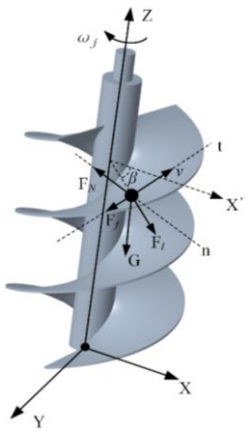

Figure 3: The stress of the particles.

The forces of the particle in the X, Y, and Z directions are expressed as follows:

$$\begin{cases} F_x = \left(F_N \sin\lambda + F_f \cos\lambda\right)\sin\beta + F_l \cos\beta \\ F_x = ma_x \\ F_y = \left(F_N \sin\lambda + F_f \cos\lambda\right)\cos\beta - F_l \sin\beta \\ F_y = ma_y \\ F_z = F_N \cos\lambda - G - F_f \sin\lambda \\ F_Z = ma_z \end{cases} \tag{4}$$

According to Eqs. (3) and (4), the motion equation of the particles in the OXYZ coordinate system can be obtained.

$$\begin{cases} \dfrac{d^2x}{dt^2} = A_1 \dfrac{dx}{dt} + B_1 \\ \dfrac{d^2y}{dt^2} = C_1 \dfrac{dy}{dt} + D_L \\ \dfrac{d^2z}{dt^2} = E_1 \dfrac{dz}{dt} + T_1 \end{cases} \tag{5}$$

Through the analysis of Eqs. (3) to (5), it is determined that the main factors affecting the movement of the particle on the spiral auger blade are the spiral angle, angular velocity of the spiral auger, and friction coefficient between the particle and spiral auger.

Blade angle of spiral augers: When the soil and fertilizer particles are stirred and mixed, a relative motion is observed not only in the spiral auger but also between the particles. When the action between the particle and spiral auger is considered, the upper and lower relative motion of the soil and fertilizer particles under the action of the spiral auger should also be considered. Hence, the following can be obtained by combining Eq. (4):

$$\begin{cases} F_z = mg\sin^2\lambda + \dfrac{1}{2}\mu mg\sin 2\lambda \\ 0 < F_Z \\ \min\left\{F_{zT}, F_{zF}\right\} \le F_z \le \max\left\{F_{zT}, F_{zF}\right\} \end{cases} \tag{6}$$

where F_{zT} is the component force of the soil particles on the z-axis, F_{zF} is the component force of the fertilizer particles on the z-axis, μ is the friction coefficient between the soil particles and spiral auger.

In this study, the spiral auger is made of steel. Based on the relevant literature, the parameters are substituted into Eq. (6) to obtain the following:

$$11.3° \le \lambda \le 21.8° \tag{7}$$

Rotation speed of spiral auger: The rotation speed of the auger has a considerable influence on the fertilizer-soil mixing operating effect. In the fertilizer-soil mixing process, the fertilizer particles and soil particles undergo spatial compound motion within the rotating range of the auger, and the particles move linearly not only along the axis of the auger but also in the forward direction of the machine. The particle movement is affected by not only the spiral auger blade but also the interaction between the particles and centrifugal force. To achieve an improved fertilizer-soil mixing effect and low power consumption in the mixing operation, the particles should not be tossed out during the mixing, and the critical rotation speed of the spiral auger should be calculated. According to the above conditions, the following can be derived through Eqs. (3) to (6):

$$\begin{cases} n \le \dfrac{30}{\sqrt{c}}\sqrt{\sin\lambda - \mu\cos\lambda\sin\delta} \\ \delta = \arctan\mu \end{cases} \tag{8}$$

The friction coefficient between the fertilizer particles and steel is 0.4, the friction coefficient between the soil particles and steel is 0.2, and the range of the spiral angle (λ) of the spiral auger blade is substituted into Eq. (8), and the range of the rotation speed of the spiral auger is calculated as 31.3-60.9 r/min. To facilitate the simulation test, the rotation speed is rounded off to 30-61 r/min.

3.3 Fertilizer mixing process simulation of fertilizer-soil mixing device

Parameter setting: The simulation test of the fertilizer-soil mixing device is based on the test results of the fertilizer discharging process; thus, only the characteristic parameters of the steel material and static and dynamic friction coefficients and collision recovery coefficients between the fertilizer particles and steel and those between the soil particles and steel are increased. Based on the related literature [19, 20], the parameters of the fertilizer-soil mixing process simulation test are shown in Table I.

Table I: Material characteristic parameters.

Property	Parameter	Value
Soil	Density ρ (kg/m^3)	1638
	Elasticity modulus G (Pa)	1.15×10^7
	Poisson's ratio ν	0.30
Fertilizer	Density ρ (kg/m$^{3)}$	1335
	Elasticity modulus G (Pa)	1.00×10^7
	Poisson's ratio ν	0.23
Steel	Density ρ (kg/m$^{3)}$	7850
	Elasticity modulus G (Pa)	7.90×10^{10}
	Poisson's ratio	0.30
Soil-soil	Static friction coefficient	0.20
	Dynamic friction coefficient	0.30
	Recovery coefficient	0.15
Soil-Fertilizer	Static friction coefficient	1.26
	Dynamic friction coefficient	1.20
	Recovery coefficient	0.02
Soil-Steel	Static friction coefficient	0.20
	Dynamic friction coefficient	0.02
	Recovery coefficient	0.10
Fertilizer-Fertilizer	Static friction coefficient	0.34
	Dynamic friction coefficient	0.16
	Recovery coefficient	0.35
Fertilizer-Steel	Static friction coefficient	0.40
	Dynamic friction coefficient	0.02
	Recovery coefficient	0.50

Modelling and mesh division: Based on the above analysis, the maximum and minimum soil thickness for the fertilizer-soil mixing operation are 0.4 m and 0.2 m, respectively. Hence, furrow models with a soil thickness of 0.2 m and 0.4 m are established.

In the EDEM (Discrete Element Method) simulation analysis, to shorten the simulation time and improve the test efficiency, the device model is appropriately simplified after the parts and components that can have a minor influence on the simulation test results. According to the actual situation of furrows and agronomic requirements of orchard furrowing fertilization, the sampling area is subjected to mesh generation. In the soil-bearing area, a statistical area with 12 lines, 8 columns, and 4 rows (soil thickness of 20 cm) and another area with 12 lines, 8 columns, and 8 rows (soil thickness of 40 cm) are arranged. The size of each mesh is 50 mm ×

50 mm × 50 mm, and the forward direction of the device is set to the longitudinal direction. The mesh generation of the sampling area is displayed in Fig. 4.

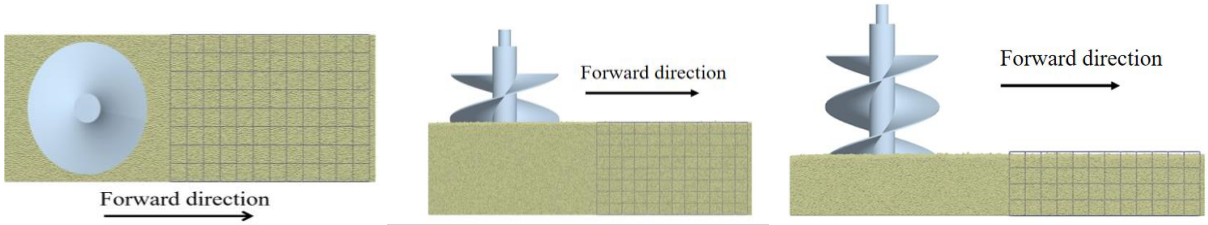

a) the longitudinal direction b) soil thickness of 40 cm c) soil thickness of 20 cm

Figure 4: Mesh generation.

Operation index of fertilizer-soil mixing device: When the operating effect of the fertilizer-soil mixing device is evaluated, the fertilizer-soil mixing uniformity should be analysed quantitatively. Based on the relevant literature [21] and actual situation in this study, the Lacey index is chosen as the evaluation index for the operating effect of the fertilizer-soil mixing device. The Lacey index is calculated as follows:

$$M = \frac{S_0^2 - S^2}{S_0^2 - S_R^2} \tag{9}$$

where S_0^2 is the variance in the complete separation system, S^2 is the actual variance of the mixture, S_R^2 is the variance in the complete mixing system.

4. RESULTS ANALYSIS AND DISCUSSION

4.1 Experimental scheme and data statistics

To further study the influencing laws of the spiral angle of the spiral auger blade, rotation speed of the spiral auger, and their interaction term and quadratic term on the operating effect of the fertilizer-soil mixing device, on the basis of the single-factor test, an orthogonal combination test was conducted to investigate the influence of the spiral auger on the fertilizer-soil mixing uniformity. The test factors were coded, as seen in Table II.

Table II: The coding level of factor.

Coding	**The spiral angle λ** (°)	**The rotation speed of the spiral auger n** (r/min)
-1	13.93	37.75
0	16.55	45.5
1	19.18	53.25

The test scheme and results are shown in Table III.

4.2 Analysis of experimental results

Analysis of variance: The evaluation index, namely, the Lacey index, to study the fertilizer-soil mixing uniformity was subjected to quadratic regression fitting analysis via Design-Expert. Based on the analysis, the regression equation of the Lacey index was acquired, followed by the analysis of variance and significance analysis of its quadratic regression model. The analysis of variance of the Lacey index at a soil thickness of 20 cm is presented in Table IV.

Table III: The test scheme and results.

Serial number	λ (°)	***n*** (r/min)	***M*** (20 cm)	***M*** (40 cm)
1	13.93	37.75	0.82	0.76
2	13.93	45.5	0.86	0.80
3	16.555	45.5	0.94	0.83
4	16.555	45.5	0.93	0.85
5	19.18	37.75	0.79	0.84
6	19.18	53.25	0.83	0.89
7	16.555	45.5	0.93	0.81
8	13.93	53.25	0.76	0.81
9	16.555	45.5	0.93	0.84
10	16.555	53.25	0.84	0.87
11	16.555	45.5	0.93	0.85
12	16.555	37.75	0.87	0.81
13	19.18	45.5	0.90	0.87

Table IV: Analysis of variance of mixing uniformity at soil thickness of 20 cm.

Source	**Quadratic sum**	**Freedom**	**Mean square**	***F***	***P***
Model	0.043	5	0.0087	172.25	＜0.0001***
λ	0.0029	1	0.0011	57.01	0.0025***
n	0.0004	1	0.0004	8.27	0.0238**
λn	0.0025	1	0.0025	49.59	0.0002***
λ^2	0.0079	1	0.0079	156.51	＜0.0001***
n^2	0.017	1	0.017	337.17	＜0.0001***
Residual error	0.0004	7	0.00005		
Lack-of-fit	0.0003	3	0.00009	4.55	0.0887*
Error	0.00008	4	0.00002		
Total	0.044	12			

Note: *** indicates that the influence is extremely significant ($P \leq 0.01$), ** indicates that the influence is significant ($0.01 < P \leq 0.05$), and * indicates that the influence is not significant ($0.05 < P$); the same below.

It can be seen in Table IV that the lack-of-fit term satisfied $P > 0.05$, indicating an insignificant influence and that the model could correctly reflect the relationship between each factor and the error and predict the test results. The influence of each factor on the Lacey index was sorted in descending order as the spiral angle and rotation speed of the spiral auger.

At a soil thickness of 20 cm, the quadratic polynomial regression equation between the Lacey index M and each factor is shown in Eq. (10).

$$M = 0.93 + 0.013\,\lambda - 0.0083\,n + 0.025\,\lambda n - 0.053\,\lambda^2 - 0.078\,n^2 \quad (10)$$

The analysis of variance of the Lacey index at a soil thickness of 20 cm is shown in Table V. It can be seen in Table V that the lack-of-fit term satisfied $P > 0.05$, indicating an insignificant influence and that the model could correctly reflect the relationship between each factor and the error and predict the test results. The influence of each factor on the Lacey index was sorted in descending order as the spiral angle λ and rotation speed of the spiral auger.

Table V: Analysis of variance of mixing uniformity at soil thickness of 20 cm.

Source	Quadratic sum	Freedom	Mean square	*F*	*P*
Model	0.013	5	0.0027	14.14	0.0015***
λ	0.0088	1	0.0088	46.69	0.0002***
n	0.0043	1	0.0043	22.59	0.0021**
λn	0.000	1	0.000	0.00	1.0000*
λ^2	0.0002	1	0.0002	0.88	0.3793*
n^2	0.00002	1	0.00002	0.11	0.7484*
Residual error	0.0013	7	0.0002		
Lack-of-fit	0.0002	3	0.00007	0.24	0.8645*
Error	0.0011	4	0.0003		
Total	0.015	12			

At a soil thickness of 40 cm, the quadratic polynomial regression equation between the Lacey index *M* and each factor is shown in Eq. (11).

$$M = 0.84 + 0.038\,\lambda + 0.027\,n - 0.0078\,\lambda^2 - 0.0028\,n^2 \quad (11)$$

Response curve analysis: The influence of the interaction between the spiral angle and rotation speed of the spiral auger on the Lacey index at different soil thicknesses was determined by processing the test results, and its response surface is shown in Fig. 5.

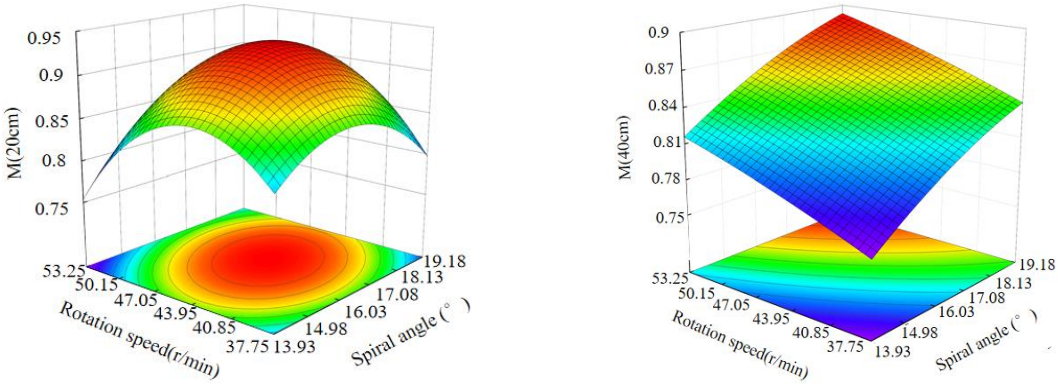

a) *M* = 20 cm (λ, *n*) b) *M* = 40 cm (λ, *n*)

Figure 5: Response surface.

As shown in Fig. 5 a, when the spiral angle was fixed and the rotation speed was within 37.75–45.5 r/min, the Lacey index increased as the rotating speed of the spiral auger increased. Within 45.5–53.25 r/min, the Lacey index showed a declining trend as the rotation speed increased. At a fixed rotation speed, the Lacey index first increased, then declined as the spiral angle increased within the test range. As shown in Fig. 5 b, at a fixed spiral angle, the Lacey index grew as the rotation speed of the spiral auger increased within the value range. When the rotation speed was fixed, the Lacey index increased as the spiral angle increased within the test range, basically showing a positive correlation trend.

Soil disturbance analysis: when the Lacey index method was used, to avoid the change in the variance toward an inaccurate range, if the total number of particles in one unit was smaller than the average number of particles in the same unit, then the unit was excluded. Hence, the soil distribution before and after the fertilizer-soil mixing operation cannot be judged quantitatively by the Lacey index method, and the soil disturbance should be analysed independently. After the mixing completion of the spiral auger, particle height distribution nephograms at a soil thickness of 40 cm and 20 cm are displayed in Figs. 6 and 7.

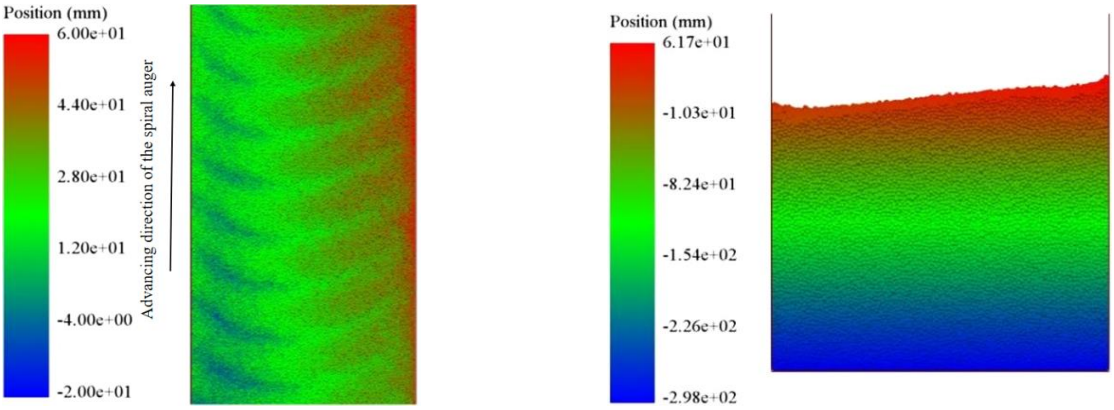

a) Advancing direction of the auger b) Sectional direction of the furrow

Figure 6: Particle height distribution nephograms at a soil thickness of 40 cm.

In Fig. 6 a, with the movement of the spiral auger, the particle height in the advancing direction of the auger presented a corrugated distribution. Owing to the influence of the rotating direction of the spiral auger, the accumulation area of the particles changed gradually from the left side to the right side of the advancing direction, the concave area on the left side recovered gradually, and the height difference between the two sides decreased gradually and tended to be balanced at the end of the fertilizer-soil mixing operation. In Fig. 6 b, influenced by the spiral auger, the particles accumulated on the right side of the furrow, presenting a distribution pattern of low on the left side and high on the right side, mainly because the particles were affected by the rotation speed and direction of the spiral auger and had a certain initial velocity when breaking away from the spiral auger. Consequently, the particles accumulated on the right side of the furrow.

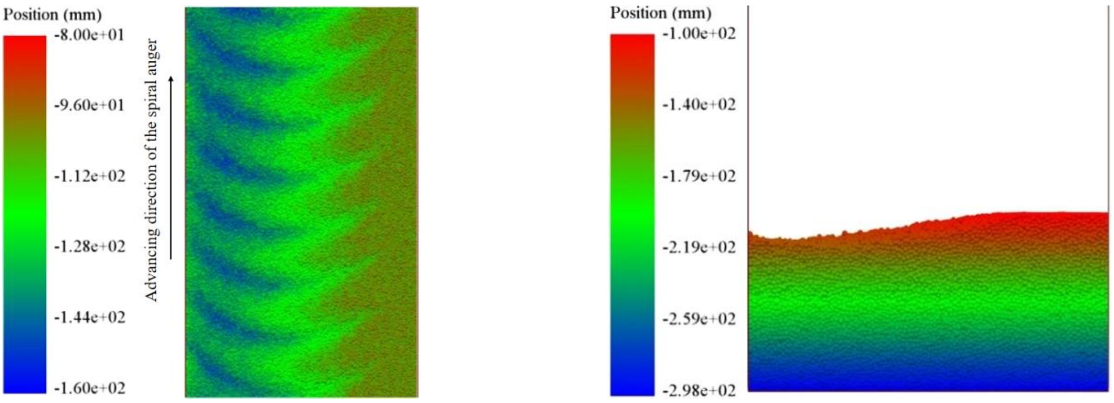

a) Advancing direction of the auger b) Sectional direction of the furrow

Figure 7: Particle height distribution nephograms at a soil thickness of 20 cm.

It can be seen in Fig. 7 a that with the movement of the spiral auger, the particle height in the advancing direction of the spiral auger also presented a corrugated distribution, and as the spiral auger rotated, the distribution in the particle accumulation area showed nearly no evident changes, without apparent changes in the height difference on the two sides. As shown in Fig. 7 b, in the sectional direction of the furrow, the particle height distribution law at a soil thickness of 20 cm was identical to that at a soil thickness of 40 cm, showing a distribution law of low on the left side and high on the right side.

Parameter optimization: The established quadratic regression equation was analysed and optimized via Design-Expert, and the optimal parameter combination was a spiral auger spiral angle of 18.12° and rotation speed of 47.67 r/min. The Lacey index predicted by the model was 0.92 at a soil thickness of 20 cm and 0.84 at a soil thickness of 40 cm.

5. CONCLUSION

To address the problem of root burning and low fertilization quality caused by the traditional orchard furrowing fertilization machines, a fertilizer mixing device was explored by combining a theoretical design with discrete elements. The following conclusions were drawn:

(1) The main structural parameters of the spiral auger were determined by the theoretical design, and the force condition of the particles on the spiral auger was analysed. Next, the main factors that may influence the motion of the particles were determined, a single-factor simulation test was conducted, and the influencing law of each factor on the fertilizer-soil mixing uniformity was determined.

(2) Through an analysis of the orthogonal combination test results of the secondary rotation, it was concluded that the spiral angle of the spiral auger blade and the rotation speed of the spiral auger exerted an extremely significant influence on the Lacey index at a soil thickness of 20 cm. At a soil thickness of 40 cm, the Lacey index was influenced, at an extremely significant level, by the spiral angle of the spiral auger blade and rotation speed of the spiral auger.

(3) Through the optimization of the established quadratic regression equation, it was determined that the optimal parameter combination was a spiral auger spiral angle of 18.12° and rotation speed of 47.67 r/min. The Lacey index predicted by the model was 0.92 at a soil thickness of 20 cm and 0.84 cm at a soil thickness of 40 cm.

In this study, a spiral auger was applied to the fertilizer mixing operation of furrowing fertilization, which can solve the problem of root burning caused by excessive fertilizer use while enhancing the uniformity of furrow-bottom fertilizer distribution. The study results can be of considerable significance to the mitigation of environmental pollution and improvement of orchard yield and fruit quality.

ACKNOWLEDGEMENT

This work was supported by Doctoral Startup Fund of the Xinjiang University (620320042), Key R & D Projects of Xinjiang Uygur Autonomous Region (2022B02028-4), and the National Natural Science Foundation of China (52265039).

REFERENCES

[1] Huinong Information. Ministry of Agriculture: Orchard Area Should be Stabilized at 200 Million Acres in 2020, from *https://news.cnhnb.com/rdzx/detail/384719/*, accessed on 10-06-2023

[2] Kilic, N.; Burgut, A.; Gundesli, M. A.; Nogay, G.; Ercisli, S.; Kafkas, N. E.; Ekiert, H.; Elansary, H. O.; Szopa, A. (2021). The effect of organic, inorganic fertilizers and their combinations on fruit quality parameters in strawberry, *Horticulture*, Vol. 7, No. 10, Paper 354, 14 pages, doi:10.3390/horticulturae7100354

[3] Sete, P. B.; Comin, J. J.; Ciotta, M. N.; Salume, J. A.; Thewes, F.; Brackmann, A.; Toselli, M.; Nava, G.; Rozane, D. E.; Loss, A.; Lourenzi, C. R.; da Rosa Couto, R.; Brunetto, G. (2019). Nitrogen fertilization affects yield and fruit quality in pear, *Scientia Horticulturae*, Vol. 258, Paper 108782, 7 pages, doi:10.1016/j.scienta.2019.108782

[4] Zheng, W.-Q.; Zhang, L.-P.; Zhang, L.-X.; Zhou, J.-P. (2020). Reflux problem analysis and structure optimization of the spiral grooved-wheel fertilizer apparatus, *International Journal of Simulation Modelling*, Vol. 19, No. 3, 422-433, doi:10.2507/IJSIMM19-3-522

[5] Zinkeviciene, R.; Jotautiene, E.; Juostas, A.; Comparetti, A.; Vaiciukevicius, E. (2021). Simulation of granular organic fertilizer application by centrifugal spreader, *Agronomy*, Vol. 11, No. 2, Paper 247, 13 pages, doi:10.3390/agronomy11020247

[6] Fulton, J. P.; Thaper, R. K.; Virk, S. S.; McDonald, T.; Fasina, O. (2020). Effect of vane shape on fertilizer distribution for a dual-disc spinner spreader, *Applied Engineering in Agriculture*, Vol. 36, No. 5, 743-751, doi:10.13031/aea.13634

[7] Sugirbay, A. M.; Zhao, J.; Nukeshev, S. O.; Chen, J. (2020). Determination of pin-roller parameters and evaluation of the uniformity of granular fertilizer application metering devices in precision farming, *Computers and Electronics in Agriculture*, Vol. 179, Paper 105835, 11 pages, doi:10.1016/j.compag.2020.105835
[8] Bandur, D.; Jaksic, B.; Bandur, M.; Jovic, S. (2019). An analysis of energy efficiency in Wireless Sensor Networks (WSNs) applied in smart agriculture, *Computers and Electronics in Agriculture*, Vol. 156, 500-507, doi:10.1016/j.compag.2018.12.016
[9] Yildirim, Y. (2006). Effect of vane number on distribution uniformity in single-disc rotary fertilizer spreaders, *Applied Engineering in Agriculture*, Vol. 22, No. 5, 659-663, doi:10.13031/2013.21998
[10] Przywara, A.; Santoro, F.; Kraszkiewicz, A.; Pecyna, A.; Pascuzzi, S. (2020). Experimental study of disc fertilizer spreader performance, *Agriculture*, Vol. 10, No. 11, Paper 575, 10 pages, doi:10.3390/agriculture10100467
[11] Villette, S.; Piron, E.; Miclet, D.; Martin, R.; Jones, G.; Paoli, J.-N.; Gee, C. (2012). How mass flow and rotational speed affect fertiliser centrifugal spreading: potential interpretation in terms of the amount of fertiliser per vane, *Biosystems Engineering*, Vol. 111, No. 1, 133-138, doi:10.1016/j.biosystemseng.2011.11.003
[12] Liu, S. X.; Xu, C. B.; Zhang, H. J.; Jiang, H.; Quan, Z. K.; Wang, J. X. (2020). Research status and development analysis of base-fertilizer application equipment of orchard, *Transactions of the Chinese Society for Agricultural Machinery*, Vol. 51, No. S2, 99-108, doi:10.6041/j.issn.1000-1298.2020.S2.012
[13] Shen, C. J.; Zhang, L. X.; Zhou, Y.; Dai, Y. M.; Li, F.; Zhang, J. (2022). Kinematic analysis and tests of the insertion mechanism of a self-propelled orchard gas explosion subsoiling and fertilizing machine, *Transactions of the Chinese Society of Agricultural Engineering*, Vol. 38, No. 1, 44-52, doi:10.11975/j.issn.1002-6819.2022.01.005
[14] Huang, Y. (2019). *Research on Ditching-fertilizing-mixing Fertilizer-back Filling Device for Orchard*, Master Thesis (in Chinese), Hebei Agricultural University, Baoding, doi:10.27109/d.cnki.ghbnu.2019.000206
[15] Sun, H. B. (2021). *Design and Experiment of Layered Variable Orchard Fertilization Machine and Key Components*, Master Thesis (in Chinese), Jilin University, Changchun, doi:10.27162/d.cnki.gjlin.2021.004878
[16] Zhang, P.-P. (2016). *The Fruit Trees Soil and Fertilizer Mixing Precision Control Fertilizer Applicator Design and Simulation*, Master Thesis (in Chinese), Shandong Agricultural University, Taian, doi:10.7666/d.D833718
[17] Cai, R.-H.; Zhao, Y.-Z. (2021). Effect of screw structure on granular mixing in a double-screw conical mixer, *Journal of Zhejiang University (Engineering Science)*, Vol. 55, No. 11, 2067-2075, doi:10.3785/j.issn.1008-973X.2021.11.006
[18] Xiao, H. R.; Zhao, Y.; Ding, W. Q.; Mei, S.; Han, Y.; Zhang, Y.; Yan, H. J.; Song, Z. Y. (2017). Design and experiment on blade shaft of 1KS60-35X type orchard double-helix trenching and fertilization machine, *Transactions of the Chinese Society of Agricultural Engineering*, Vol. 33, No. 10, 32-39, doi:10.11975/j.issn.1002-6819.2017.10.005
[19] Ahmad, F.; Qiu, B. J.; Ding, Q. S.; Ding, W. M.; Khan, Z. M.; Shoaib, M.; Chandio, F. A.; Rehim, A.; Khaliq, A. (2020). Discrete element method simulation of disc type furrow openers in paddy soil, *International Journal of Agriculture and Bioengineering*, Vol. 13, No. 4, 103-110, doi:10.25165/j.ijabe.20201304.4800
[20] Gao, K.; Li, X. H.; Gao, H. D.; Zhang, L. X.; You, F. (2023). Design and analysis of a vertical screw stirring device for feeding dairy goats, *International Journal of Simulation Modelling*, Vol. 22, No. 3, 462-473, doi:10.2507/IJSIMM22-3-655
[21] Villette, S.; Piron, E.; Miclet, D. (2017). Hybrid centrifugal spreading model to study the fertiliser spatial distribution and its assessment using the transverse coefficient of variation, *Computers and Electronics in Agriculture*, Vol. 137, 115-129, doi:10.1016/j.compag.2017.03.023